Proc. Int. Symposium on Advances in Neutron Scattering Research, Tokai, 2000
J. Phys. Soc. Jpn. **70** (2001) Suppl. A pp. 58–60

Static and Dynamical Properties of Stripes in Underdoped Cuprates

Kazushige MACHIDA, Masanori ICHIOKA and Eiji KANESHITA

Department of Physics, Okayama University, Okayama 700-8530, Japan

Static and dynamical properties of stripes realized in underdoped regions in high T_c oxide superconductors are analyzed theoretically. Based on the two-dimensional Hubbard model, we investigate the spatial spin and charge profiles of both diagonal and vertical stripes and the associated quasi-particle spectrum near the Fermi level. Recent elastic neutron and ARPES experiments on (La, Sr)$_2$CuO$_4$ and (La, Nd, Sr)$_2$CuO$_4$ are discussed in the light of the above stripe picture. Collective excitations in stripes are analyzed by evaluating the dynamical susceptibilities for the full range of energy and momentum in spin and charge channels within RPA. An intricate landscape of the spectrum and the anisotropy of low-lying collective modes; spin wave and phason are obtained.

KEYWORDS: stripe, cuprates, collective modes, spin wave, phason

§1. Introduction

The concept of the stripe structure is quite versatile and powerful in understanding various spatially modulated orderings ranging from insulator to metal, such as spin or charge density waves (SDW or CDW) or spin Peierls systems. Although the stripe concept is initially introduced via a mean-field treatment, it is believed that it is valid beyond its limitation. A canonical example of such a stripe description is the incommensurate SDW in metallic Cr dilutely doped with Mn or V atoms. Various aspects of the SDW under doping are coherently describable in terms of the stripe. Another canonical example for such description is the spin Peierls systems such as in $CuGeO_3$ or other organic materials under a magnetic field which effectively acts as changing the electron filling.

Electronic properties in underdoped high T_c cuprates arose much attention recently because it is hoped that understanding of the unusual ground state may lead us to a clue to a high T_c mechanism. However, in spite of intensive theoretical and experimental works in the past little consensus for the normal state properties has emerged yet. Recently a remarkable series of elastic neutron experiments[1] on $La_{2-x}Sr_xCuO_4$ (LSCO) has been performed, revealing static magnetic incommensurate (IC) structure: For x=0.12, 0.10, 0.08 and 0.06, which are all metallic and superconducting, the modulation vector $\mathbf{Q}$ are characterized by $\mathbf{Q} = (\frac{1}{2}, \frac{1}{2} \pm \delta)$ and $(\frac{1}{2} \pm \delta, \frac{1}{2})$ in reciprocal lattice units. The IC modulation runs vertically in the a (b)-axis of the CuO_2 plane. For x=0.05$\sim$ 0.03 which are insulating the above four superspots rotate by 45° around the $(\frac{1}{2}, \frac{1}{2})$ position, characterized by $(\frac{1}{2} \pm \delta, \frac{1}{2} \pm \delta)$. The IC modulation is now in the diagonal direction. The incommesurability δ is given by $\delta = x$ for $0.05 \leq x \leq 0.12$ beyond which δ saturates.

In the further dilute region ($0 < x \leq 0.02$) upon lowering T the antiferromagnetic (AF) phase changes into a "spin-freezing" structure at the Johnston line given by T_f=815x (K), below which the internal magnetic field probed by the La-NQR is mysteriously broaden.[2]

The static magnetic structures in superconducting (La, Nd)$_{2-x}Sr_xCuO_4$ and insulating $La_{2-x}Sr_xNiO_4$ are also known. In the former Nd system[3] the vertical stripe with the same $\delta = x$ relation as in LSCO for $x > 0.07$ and in the latter Ni system the diagonal stripe with $\delta = x/2$ up to $x \simeq 0.33$ are observed.[3] Note that in YBCO vertical 1D-like IC fluctuations are also reported in inelastic neutron experiments.[4]

The purposes of this paper are to understand both static and dynamical properties of the stripes in cuprates in connection with high T_c superconductors. Based on our previous[5,6] and related works,[7] we calculate the ground state and its excitation spectrum within the mean field RPA scheme.

§2. Static Properties of Stripes

We consider the Hubbard model $H = -\Sigma_{i,j,\sigma} t_{i,j} c^\dagger_{i,\sigma} c_{j,\sigma}$ $+U\Sigma_i n_{i,\uparrow} n_{i,\downarrow}$ in two dimensions where $t_{i,j} = t$ for the nearest neighbor pairs (i,j) and $t_{i,j} = t'$ for the next nearest neighbor pairs situated on a diagonal position in a square lattice. (The energy is measured by t) The mean field $\langle n_{i,\sigma} \rangle = n_i + \sigma M_i$ at i-site is introduced where $n_i(M_i)$ is the charge (spin) density. Thus the one-body Hamiltonian $H_{MF} = -\Sigma_{i,j,\sigma} t_{i,j} c^\dagger_{i,\sigma} c_{j,\sigma} +$ $U\Sigma_i(\langle n_{i,\uparrow} \rangle n_{i,\downarrow} + \langle n_{i,\downarrow} \rangle n_{i,\uparrow})$ is solved self-consistently in k-space under a given hole concentration or filling $1 - n_h$ per site (n_h=0 is just the half-filling), assuming a spatially periodic structure for spin and charge modulations.

After the extensive self-consistent calculations for various system parameters,[5,6] we find the followings: The incommesurability δ is given by $\delta = n_h/2$ for the insulating case where holes are accommodated in the stripe region characterized by the π-phase shift of the antiferromagnetic order. The midgap band created in between the conduction and valence bands is empty. As n_h increases, the IC pattern changes from the diagonal stripe to vertical stripe where the former (latter) tends to be insulating (metallic) as observed in LSCO. The critical hole density for the metal-insulator transition signalled

by partial occupation of the midgap band depends on the system parameters t, t' and U. In the present scheme there is no commensurate region at $T = 0$ as a function of n_h, namely, once holes are doped, IC modulation always occurs. This feature seems to be supported by the recent neutron experiment on LSCO with $n_h = 0.028$.[8] It also may explain the mysterious NQR line broadening at low dopings.[2]

In the metallic region, which is realized as n_h increases the relation δ vs n_h depends on the parameter: as $|t'|$ increases, it approaches $\delta = n_h$ whose relation is suggested experimentally in LSCO. The local density of states shows that the density of states at the Fermi level comes from the stripe region while the other antiferromagnetic region is insulating. This spatial inhomogeneity explains the anomalous Hall constant temperature behaviors[9] observed in Nd-LSCO systems. The spectral weight at the Fermi level for the metallic vertical stripe shows a characteristic parallel Fermi surfaces situated at $(\pi, 0)$ and $(0, \pi)$ positions in reciprocal space whose distance corresponds to $2k_F \sim \pi/4$ with Fermi wave number k_F, implying that the midgap band is quarter-filled. Photoemission experiments on Nd-LSCO and LSCO commonly exhibit this characteristics.[10]

§3. Dynamical Properties of Stripes

There exist a lot of theoretical works on dynamical properties for modulated SDW by Fedders and Martin,[11] Fishman and Liu[12] and others. The former first derives spin wave mode in the transverse spin excitation of itinerant electron systems. The latter investigates various transverse and longitudinal modes at the $\mathbf{Q}$ position, based on a one-dimensional (1D) model within RPA. Their theory takes account of only fundamental order parameter $M_{\mathbf{Q}}$, neglecting higher harmonics $M_{2\mathbf{Q}}$, $M_{3\mathbf{Q}}, \cdots$ associated with the incommensurability δ. Here we calculate the dynamical spin and charge susceptibilities $\chi(\mathbf{q}, \omega)$ in the full range of the two dimensional (2D) wave number $\mathbf{q}$ for entire Brillouin zone and the excitation energy ω up to the band width. We take account of all the possible higher harmonics. This will turn out to be extremely crucial in correctly evaluating these quantities. The multi-dimensional calculation here allows us to extract a wealth of information on stripe motions such as translation, or meandering, etc. and on the anisotropy of excitation cones. After constructing the thermal Green function, we evaluate the dynamical susceptibilities for various channels; the spin longitudinal mode $\chi_{zz}(\mathbf{q}, \omega) = \langle\langle S_z; S_z\rangle\rangle_{\mathbf{q},\omega}$, the transverse one $\chi_{xx}(\mathbf{q}, \omega) = \langle\langle S_x; S_x\rangle\rangle_{\mathbf{q},\omega}$, and the charge susceptibility $\chi_{nn}(\mathbf{q}, \omega) = \langle\langle n; n\rangle\rangle_{\mathbf{q},\omega}$.

The RPA equation for $\chi_{S_\uparrow S_\downarrow} = \langle\langle S_\uparrow; S_\downarrow\rangle\rangle$ is written as

$$\chi_{S_\uparrow S_\downarrow}(\mathbf{r}_1, \mathbf{r}_3, \omega) = \chi_0^{\uparrow\downarrow}(\mathbf{r}_1, \mathbf{r}_3, \omega) + U \sum_{\mathbf{r}_2} \chi_0^{\uparrow\downarrow}(\mathbf{r}_1, \mathbf{r}_2, \omega) \chi_{S_\uparrow S_\downarrow}(\mathbf{r}_2, \mathbf{r}_3, \omega). \tag{3.1}$$

After Fourier transformation to $\mathbf{k}$-space, eq. (3.1) is reduced to a matrix equation of $\chi_0^{\uparrow\downarrow}$ and $\chi_{S_\uparrow S_\downarrow}$. By solving it, we obtain $\chi_{xx}(\mathbf{k} + l_1\mathbf{Q}, \mathbf{k} + l_2\mathbf{Q}, \omega)$. In a similar manner, we calculate $\langle\langle n_\uparrow; n_\uparrow\rangle\rangle$ and $\langle\langle n_\uparrow; n_\downarrow\rangle\rangle$, and obtain $\chi_{zz}(\mathbf{k} + l_1\mathbf{Q}, \mathbf{k} + l_2\mathbf{Q}, \omega)$ and $\chi_{nn}(\mathbf{k} + l_1\mathbf{Q}, \mathbf{k} + l_2\mathbf{Q}, \omega)$. The neutron scattering experiments observe the imaginary part of the dynamical susceptibility $\chi''(\mathbf{q}, \omega) = \mathrm{Im}\chi(\mathbf{q}, \mathbf{q}, \omega)$. Since the signal is observed as spatial average, we consider the diagonal part of $\chi(\mathbf{k} + l_1\mathbf{Q}, \mathbf{k} + l_2\mathbf{Q}, \omega)$.

Let us start with the excitation of the spin transverse mode. In Fig. 2, we show $\chi''_{xx}(\mathbf{q}, \omega)$ along paths A and B of Fig. 1. The gapless spin wave modes emanate not only $\mathbf{Q}$, but also from $3\mathbf{Q}$ and other odd harmonics. The ridge of $\chi''(\mathbf{q}, \omega)$ shows singularity reflecting the dispersion of the collective mode. These modes at $(2n+1)\mathbf{Q}$ have an identical dispersion relation, because every $(2n+1)\mathbf{Q}$-modes couple each other in the RPA equation (3.1). The same dispersion pattern appears in each reduced Brillouin zone. But their intensities are different. With increasing l, the intensity is decreased as follows, $\chi''_{xx}(l\mathbf{Q}, 0.025t)/\chi''_{xx}(\mathbf{Q}, 0.025t) = 6.5 \times 10^{-3}$ $(l = 3)$, 2.7×10^{-5} $(l = 5)$, 5.8×10^{-6} $(l = 7)$. It is found that the intensity ratio is obeyed

$$\frac{\chi''_{xx}((2n+1)\mathbf{Q}, \omega \to 0)}{\chi''_{xx}(\mathbf{Q}, \omega \to 0)} \sim \left[\frac{M_{(2n+1)\mathbf{Q}}}{M_{\mathbf{Q}}}\right]^2. \tag{3.2}$$

With approaching the half-filling the above ratio is expected to increase and approach $(2n+1)^{-2}$. Then, the higher harmonics spot at $(2n+1)\mathbf{Q}$ may have enough intensity to be observed near half-fillings such as in Cr or underdoped cuprates.

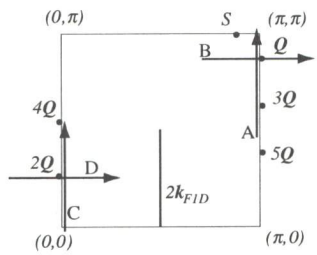

Fig. 1. The paths A-D along which we show $\chi(\mathbf{q}, \omega)$ in the momentum space. The point $\mathbf{Q}$ is the ordering vector. $2\mathbf{Q}$, $3\mathbf{Q}, \cdots$ are its higher harmonics points. $\mathbf{S}$ is the silent position. The line $2\mathbf{k}_{\mathrm{F1D}}$ shows the nesting wave number of the 1D Fermi surface in the metallic stripe state.

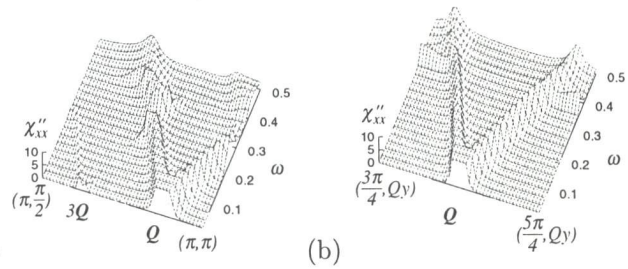

Fig. 2. Spin transverse mode $\chi''_{xx}(\mathbf{q}, \omega)$ along path A (a) and B (b). ω is scaled by t. We cut off the peak height for $\chi''_{xx} > 10$ to show the low intensity structure.

The reconnection of the dispersion curve occurs at the reduced Brillouin zone boundary. Then, instead of the simple intersection of two dispersions, the small gap ap-

pears at $\omega \sim 0.3t$ in Fig. 2. With increasing ω, the intensity of $\chi''_{xx}(\mathbf{q},\omega)$ decreases as $1/\omega$ along the dispersion curve, except for the weakened intensity at the gap position. For $\omega > E_g$ (E_g is the single particle gap), there exists other modes reflecting the fluctuation of the magnetic moment amplitude. It is a character of itinerant magnets and absent in localized spin magnets.

The spin wave velocity $v^x_{\rm spin}$ ($v^y_{\rm spin}$) is defined by the slope of the q_x- (q_y-) direction at $\omega \sim 0$. The spin modulation parallel to the stripe (domain wall) corresponds to $v^x_{\rm spin}$. In this direction, the staggered spin moment has a constant amplitude. The modulation perpendicular to the stripe corresponds to $v^y_{\rm spin}$. In this direction, the spin moment is modulated and suppressed when it crosses the stripe region. Since $v^x_{\rm spin} > v^y_{\rm spin}$, the spin modulation is easier for the direction perpendicular to the stripe. In other words, the effective exchange integral J across the stripe becomes weaker than that parallel to the stripe. As U increases, $v_{\rm spin}$ decreases. These results are reasonable in view of the correspondence between Hubbard and Heisenberg models: $v_{\rm spin} \sim J \propto t^2/U$. We have done the same calculation for the diagonal stripe to confirm that the spin wave velocity is similar.

The longitudinal spin mode $\chi''_{zz}(\mathbf{q},\omega)$ is shown in Fig. 3 along paths A and B of Fig. 1. Low energy modes appears at $(2n+1)\mathbf{Q}$. Along path A, the dispersion relation is continuous and repeated, touching at $(2n+1)\mathbf{Q}$. Away from $\mathbf{Q}$, the intensity decreases as $\chi''_{zz}(l\mathbf{Q}, 0.01t)/\chi''_{zz}(\mathbf{Q}, 0.01t) = 5.9 \times 10^{-2}$ ($l = 3$), 6.9×10^{-4} ($l = 5$), 5.3×10^{-4} ($l = 7$). These ratios are larger than those given by Eq. (3.2), which is, thus, not satisfied for χ_{zz}. The intensity $\chi''_{zz}(\mathbf{q},\omega) \sim \frac{1}{3}\chi''_{xx}(\mathbf{q},\omega)$ near $\mathbf{Q}$ along each dispersion relation in our results. There, $\chi''_{zz}(\mathbf{q},\omega) \sim 1/\omega$ with increasing ω.

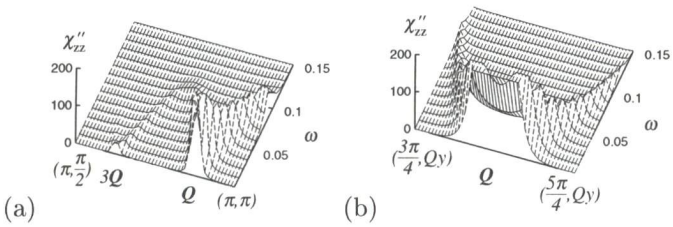

Fig. 3. Spin longitudinal mode $\chi''_{zz}(\mathbf{q},\omega)$ along path A (a) and B (b). We cut off the peak height for $\chi''_{zz} > 200$.

The charge mode $\chi''_{nn}(\mathbf{q},\omega)$ is shown in Fig. 4 along paths C and D of Fig. 1. The low energy mode appears at $2n\mathbf{Q}$. It has the identical dispersion curve as that of χ_{zz}, because S_z and n couple each other in the RPA equation. As in Fig. 4 (a), it is a continuous curve along path C and its intensity deceases away from $2\mathbf{Q}$. The $2\mathbf{Q}$ mode comes from even harmonics, as $\langle n_{2\mathbf{Q},\sigma}\rangle$ describes the charge modulation in the ISDW.

So far we mention only the insulating stripe state. The corresponding metallic stripe state can be also stabilized by merely introducing the next nearest hopping t'. The lowest energy state is given by $\delta \sim n_{\rm h}$, and the Fermi level situates in the so-called midgap band.[6] Since $v^y_{\rm spin}$ increases and $v^x_{\rm spin}$ decreases, we find $v^y_{\rm spin} > v^x_{\rm spin}$ in χ''_{xx}. There is low energy excitation also at $\mathbf{S}$. In χ''_{zz}

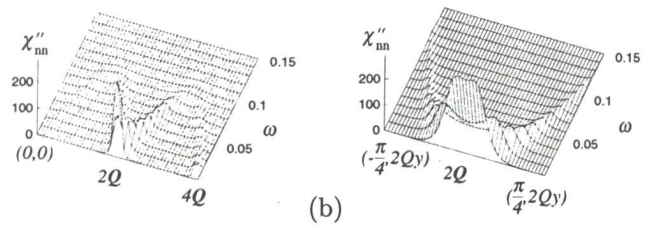

Fig. 4. Charge mode $\chi''_{nn}(\mathbf{q},\omega)$ along path C (a) and D (b).

and χ''_{nn}, the excitation at $\mathbf{Q}$ or $2\mathbf{Q}$ has a gap. The low energy excitation appears along the line at $q_x = \pi/2$ which is presented by a line in Fig. 1. It is the 1D CDW or SDW fluctuation mode within the stripe line, and originated from the Fermi surface nesting $2\mathbf{k}_{\rm F1D}$ of the parallel 1D Fermi lines of the stripe state.[10] Since the 1D Fermi state has a gap near $(\frac{\pi}{2},\frac{\pi}{2})$, the intensity of $\chi''(2\mathbf{k}_{\rm F1D},\omega \sim 0)$ vanishes near $(\frac{\pi}{2},\pi)$. These low energy excitations are diffusive since $E_g = 0$ in metallic state.

§4. Conclusion

We investigated the static and dynamical properties of stripes realized in some of the high T_c cuprates within HFA-RPA scheme. It is pointed out that the predicted static features are observed experimentally; commensurate-incommensurate cross-over on lowering T and 1D-like parallel Fermi surface in LSCO. Dynamical susceptibilities of transverse and longitudinal spin channels and charge one for the whole space spanned by 2D wave vector $\mathbf{q}$ and the energy ω are investigated. We identified several elementary excitations; the spin wave mode and the phason mode related to the motion of the stripe line. This allows us to construct the whole landscape of $(\mathbf{q},\omega)$ space for the excitation spectra of various channels: The identical dispersion relation is replicated at every $(2n+1)\mathbf{Q}$, which has the anisotropic excitation cones along q_x- and q_y-directions. Our predictions about $\chi(\mathbf{q},\omega)$ are directly testable by careful inelastic neutron experiments on Cr alloys and underdoped cuprates.

1) S. Wakimoto *et al.*: Phys. Rev. B. **61** (2000) 851; S. Wakimoto *et al.*: preprint; T. Suzuki *et al.*: Phys. Rev. B**57** (1998) R3229.
2) J.H. Cho *et al.*: Phys. Rev. Lett. **70**(1993) 222; F.C. Chou *et al.*: *ibid* **71** (1993) 2323.
3) J.M.Tranquada *et al.*: Phys. Rev. Lett. **78** (1997) 338.
4) H. Mook *et al.*: Nature **395** (1998) 580; *ibid* **404** (2000) 729.
5) K. Machida: Physica C **158** (1989) 192; M. Kato *et al.*: J. Phys. Soc. Jpn. **59** (1990) 1047.
6) K. Machida and M. Ichioka: J. Phys. Soc. Jpn. **68** (1999) 2168; M. Ichioka and K. Machida: *ibid* **68** (1999) 4020.
7) D. Poilblanc and T.M. Rice: Phys. Rev. B**39** (1989) 9749; J. Zaanen and O. Gunnarsson: *ibid* B**40** (1990) 7391; H. Schulz: Phys. Rev. Lett. **64** (1990) 1445.
8) M. Matsuda *et al.*: private communication.
9) T. Noda *et al.*: Science **286** (1999) 265.
10) X.J. Zhou *et al.*: Science **286** (1999) 268; A. Ino *et al.*: J. Phys. Soc. Jpn. **68** (1999) 1496.
11) P. A. Fedders and P.C. Martin: Phys. Rev. **143** (1966) 1845.
12) R.S. Fishman and S.H. Liu: Phys. Rev. B **54** (1996) 7233 and 7252.